Adsorption (2013) 19:131–142
DOI 10.1007/s10450-012-9433-z

On the description of isotherms of CH_4 and C_2H_4 adsorption on graphite from subcritical to supercritical conditions

Reconciliation between computer simulation and experimental data

Mus'ab Abdul Razak · D.D. Do · Toshihide Horikawa · Keita Tsuji · D. Nicholson

Received: 6 August 2012 / Accepted: 24 September 2012 / Published online: 3 October 2012

Abstract Different potential models for methane and ethylene are tested for their suitability for the description of bulk phase behavior, including coexistence, and adsorption on a graphite surface under sub- and super-critical conditions using GCMC simulation. Under sub-critical conditions, those intermolecular potential models that describe correctly the vapor–liquid equilibria were found to be adequate for the description of surface adsorption. These potential models can also give a good account of adsorption under supercritical conditions or near-critical conditions, provided the experimental data (in terms of excess) are correctly obtained with the reliably determined void volume as illustrated in this paper with methane adsorption.

Keywords Adsorption · Graphon · Methane · Ethylene · Supercritical

Electronic supplementary material The online version of this article (doi:10.1007/s10450-012-9433-z) contains supplementary material, which is available to authorized users.

M. Abdul Razak · D.D. Do (✉) · D. Nicholson
School of Chemical Engineering, University of Queensland, St. Lucia, Qld 4072, Australia
e-mail: d.d.do@uq.edu.au

T. Horikawa
Department of Advanced Materials, Institute of Technology and Science, The University of Tokushima, 2-1 Minamijosanjima, Tokushima 770-8506, Japan

K. Tsuji
BEL Japan, inc., Osaka 561-0807, Japan

1 Introduction

Adsorption of gases under supercritical conditions has attracted good interest recently, by many research groups, both experimentally and theoretically because of its importance in applications such as energy storage of natural gas and hydrogen (Poirier et al. 2001; Malbrunot et al. 1996; Darkrim et al. 2002). Experimental studies of these gases and other gases are abundant in the literature; for example, Zhou et al. (2002) studied methane and nitrogen adsorption from sub- to supercritical region on silica gel, and Malbrunot et al. (1992) studied the adsorption of argon, krypton, neon, nitrogen and methane on activated carbon above the critical point region using a dielectric method. While Salem et al. (1998) dealt with adsorption of argon, nitrogen and methane on 13X molecular sieve and activated carbon over a wide range of temperatures and pressures.

Theoretical studies of supercritical fluids stem from not only the importance of energy storage but also the need to understand better the various interesting behaviors observed under supercritical conditions; for example, the existence of a maximum in the adsorption isotherm (plotted as surface excess versus pressure) (Menon 1968; Ozawa et al. 1976; Specovius and Findenegg 1978; Jiang et al. 1994). With the use of molecular simulation methods such as Monte Carlo (MC), Molecular Dynamics (Allen and Tildesley 1989; Nicholson and Parsonage 1982; Frenkel and Smit 1996) (MD) and Density Functional Theory (DFT) (El-Merraoui et al. 2000; Tanaka et al. 2002; Ustinov 2009), adsorption of gases on non-porous surfaces is understood especially at temperatures below the critical points, but there is a need for further research in supercritical adsorption, especially the reconciliation between the simulation results and experimental data. Many relevant theoretical and simulation papers have appeared in the past two decades using

Monte Carlo (Do and Do 2005a; Tan and Gubbins 1990; Matranga et al. 1992; Darkrim et al. 1999; Kowalczyk et al. 2005), DFT (Jiang et al. 1994; Murata et al. 2001; Ustinov and Do 2003), Ono-Kondo analysis (Aranovich and Donohue 1996; Hocker et al. 2003; Gao et al. 2004), and empirical or semi-empirical approaches (Murata et al. 2001; Kaneko and Murata 1997; Agarwal and Schwarz 1988).

We have studied adsorption of many gases on graphite under sub-critical conditions using Monte Carlo simulation (Do and Do 2005b; Nguyen et al. 2010; Abdul Razak et al. 2011), and have found that those potential models that describe the vapor-liquid equilibria well are also suitable for the description of adsorption. In this paper, we chose methane and ethylene as model adsorbates to study their adsorption over a wide range of conditions, from sub-critical to near-critical and supercritical. Experimental data for these gases on graphite surfaces over a wide range of temperature are available in the literature (Specovius and Findenegg 1978, 1980; Avgul and Kiselev 1970).

2 Theory

The different potential models available in the literature that can be used to describe dispersive, repulsive and electrostatic interactions for methane and ethylene, are listed in Table 1.

The interaction energy between a site a on a molecule i with a site b on a molecule j is calculated with the following Lennard-Jones 12-6 equation:

$$\varphi_{i,j}^{(a,b)} = 4\varepsilon^{(a,b)}\left[\left(\frac{\sigma^{(a,b)}}{r_{i,j}^{(a,b)}}\right)^{12} - \left(\frac{\sigma^{(a,b)}}{r_{i,j}^{(a,b)}}\right)^{6}\right] \tag{1}$$

The Lorentz-Berthelot (LB) mixing rules are used to obtain the cross collision diameter $\sigma^{(a,b)}$ and the cross well-depth $\varepsilon^{(a,b)}$. The interaction between a charge α on a molecule i and a charge β on a molecule j is determined via the Coulomb law of electrostatic interaction:

$$\varphi_{q;i,j}^{(\alpha,\beta)} = \frac{1}{4\pi\varepsilon_0}\cdot\frac{q_i^{\alpha}q_j^{\beta}}{r_{i,j}^{(\alpha,\beta)}} \tag{2}$$

where ε_0 is the permittivity of free space ($\varepsilon_0 = 8.8543 \times 10^{-12}\ \mathrm{C^2\,J^{-1}\,m^{-1}}$).

The solid-fluid potential between a site i and the surface is calculated with the Steele 10-4-3 equation (Steele 1973).

$$\varphi_{i,S} = \varphi_W\left[\frac{1}{5}\left(\frac{\sigma^{(a,c)}}{z_i}\right)^{10} - \frac{1}{2}\left(\frac{\sigma^{(a,c)}}{z_i}\right)^{4} - \frac{(\sigma^{(a,c)})^4}{6\Delta(z_i+0.61\Delta)^3}\right] \tag{3}$$

Here the wall potential energy parameter φ_W is given by $\varphi_W = 4\pi\rho_s\varepsilon^{(a,c)}[\sigma^{(a,c)}]^2$, where ρ_s is the density of carbon atoms per unit surface area ($\rho_s = 38.2\ \mathrm{nm^{-2}}$). The solid-fluid well-depth of the interaction energy is calculated from the following equation, $\varepsilon^{(a,c)} = (1-k_{SF})\cdot\sqrt{\varepsilon^{(a,a)}\cdot\varepsilon^{(c,c)}}$, where a and c denote adsorbate and carbon, respectively, and k_{SF} is the binary interaction parameter. The molecular parameters of the carbon atom in graphite are $\sigma = 0.34$ nm and $\varepsilon/k_B = 28$ K.

2.1 Adsorption surface excess

The surface excess of adsorption is defined as the excess above a reference amount, given by:

$$\Gamma = \frac{\langle N\rangle - V'\rho_b}{A} \tag{4}$$

where $\langle N\rangle$ is the ensemble average of the number of particle in the simulation box, V' is the void volume, ρ_b is the bulk density and A is the area of the graphite wall. Since the two terms on the RHS of Eq. (4) are comparable under supercritical conditions, the reliability of the calculated surface excess depends critically on the accuracy of the void volume and the bulk gas density. Assuming the bulk gas density is accurately known or calculated from a reliable equation of state, the issue lies with the void volume, and we shall show below how important this is for methane adsorption on graphite under supercritical conditions.

The void volume is commonly determined experimentally by helium expansion; to have a direct comparison between the simulation and experimental data we need to determine the helium void volume by carrying out simulation of helium adsorption at 1 atm and ambient temperature. By assuming zero excess of helium (as is also assumed in experimental calculations), the He-void volume can be calculated, as the average number of helium molecules in the simulation box divided by the helium density (from Eq. (4)).

2.2 Grand canonical Monte Carlo simulation

The molecular simulations were carried out using Grand Canonical Monte Carlo (GCMC) (Allen and Tildesley 1989; Frenkel and Smit 1996). The MC parameters used in this paper are: (i) the box lengths in the x- and y-directions were at least 15 times the collision diameter, (ii) the cut off radius for the calculation of the potential energy was either five times the collision diameter or half the shorter linear dimension of the box, and (iii) the number of cycles for equilibration and sampling steps was 50,000, with 1000 displacement, insertion and deletion moves in each cycle chosen with equal probability. Periodic boundary conditions were imposed at the boundaries in the x and y directions. In the z direction,

Table 1 Molecular parameters of methane and ethylene

Adsorbates			σ (nm)	ε/k_B (K)	q (e)	Q^{2*} (–)	$l_{\text{C-C}}$ (nm)	$l_{\text{C-H}}$ (nm)	$\theta_{\text{H-C-H}}$ (°)	δ[a] (nm)	Ref.
Methane	TraPPE	CH_4	0.373	148.00							Martin and Siepmann (1998)
	Steele	CH_4	0.381	148.10							Steele (1973)
	Ohba	CH_4	0.372	161.30							Ohba et al. (2004)
	Sun	C	0.340	55.06	−0.660			0.109	109.5		Sun et al. (1992)
		H	0.265	7.90	0.165						
Ethylene	TraPPE	CH_3	0.368	85.00			0.154				Wick et al. (2000)
	AUA-4	CH_3	0.348	111.10			0.154			0.0295	Bourasseau et al. (2003)
	Vrabec	CH_3	0.376	76.95		2.347	0.127				Vrabec et al. (2001)
	NERD	CH_3	0.379	84.70			0.154				Nath et al. (2001)
	SET	CH_3	0.363	91.40			0.148				Spyriouni et al. (1998)
	OPLS-AA	C	0.355	38.27	−0.230		0.133	0.109	117.4		Jorgensen et al. (1996)
		H	0.242	15.11	0.115						

[a] δ is the carbon to centre distance

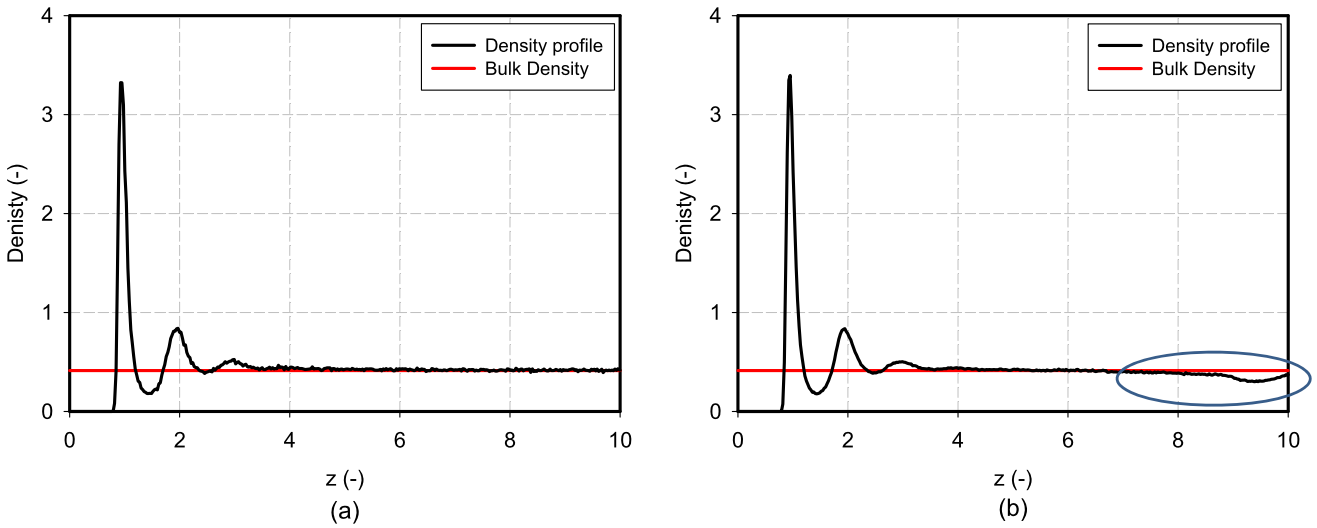

Fig. 1 Density profile of methane adsorption at 298 K and 30 MPa (**a**) using two independent surfaces, and (**b**) using one surface and a hard wall at the boundaries

both ends were terminated by a graphite surface at a distance of at least 20 (for methane) and 30 times (for ethylene) the collision diameter. This ensures that the system behaves as two independent surfaces and the fluid in the middle of the pore behaves as a bulk fluid. The alternative of using a hard wall at one boundary in the z-direction, has a spurious effect on the density profile especially when we deal with supercritical adsorption, as shown in the local density profile of methane adsorption at 298 K and 30 MPa in Fig. 1. The highlighted area Fig. 1b indicates the spurious effect at the hard wall boundary while such effect is absent when two surfaces were used as shown in Fig. 1a.

2.3 Gibbs ensemble Monte Carlo simulation

The phase coexistence of vapor and liquid equilibrium was determined using Gibbs ensemble MC with two unconnected simulation boxes (Frenkel and Smit 1996; Panagiotopoulos et al. 1988). In this simulation, there are three moves: One is the displacement and rotation of molecules in each box, the second is the interchange of a particle between the two boxes, and the third is the volume change while maintaining the total volume constant. The probabilities for these three moves were 0.333, 0.665, and 0.002, respectively.

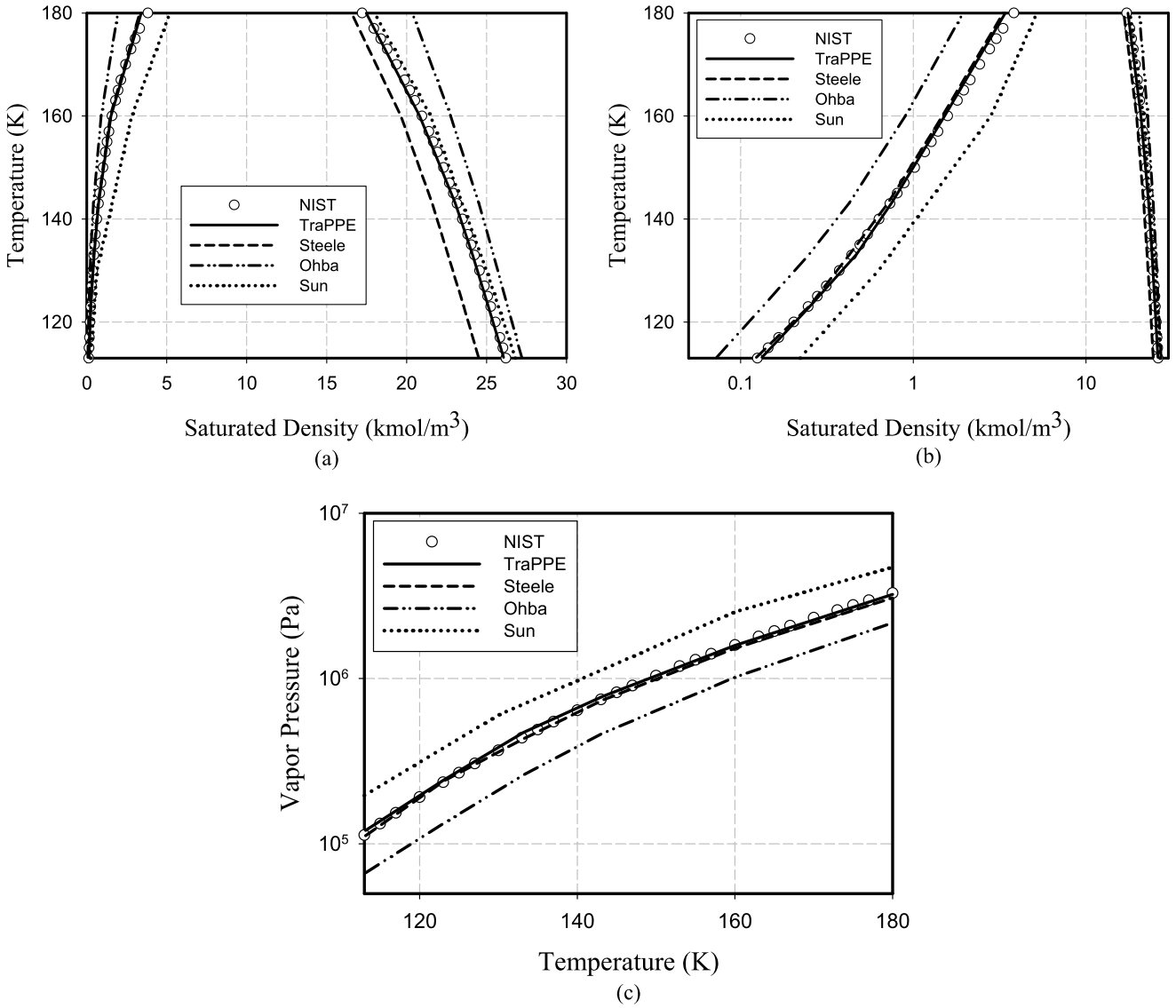

Fig. 2 VLE phase diagrams for methane: (**a**) linear scale of density (*top LHS*) and (**b**) log scale of density (*top RHS*), (**c**) vapor pressures versus temperatures (*bottom*)

2.4 Isobaric-isothermal Monte Carlo simulation

The bulk behavior was determined using the isobaric-isothermal ensemble MC (Allen and Tildesley 1989; Frenkel and Smit 1996). In this simulation, there are two moves: the displacement and rotation of the adsorbate, and volume expansion or contraction. The MC parameters used in this work were: (i) 500 particles, (ii) a cut-off radius of half of the dimension of the box for the calculation of the potential energy, and (iii) 50,000 cycles each for the equilibration and sampling steps, with 1000 displacement, insertion and deletion moves of equal probability in each cycle. Periodic boundary conditions were imposed at all boundaries.

3 Results and discussion

In adsorption systems the density distribution is not uniform; typically the smoothed density changes from high, close to the surface (liquid-like), to that of the surrounding bulk gas, and therefore the potential model for the adsorbate has to be able to describe the vapor-liquid equilibrium correctly. Previously we have shown that in the case of argon adsorption on graphite, the potential model of Michels et al. (1949), which gives a good account of the vapor-liquid equilibrium (VLE), is suitable for the description of many adsorption systems, ranging from adsorption on a graphite surface (Do and Do 2005b, 2005c) to that in the confined space of cylindrical pores (Liu et al. 2011). Here we shall further test this argument with various potential models for methane and

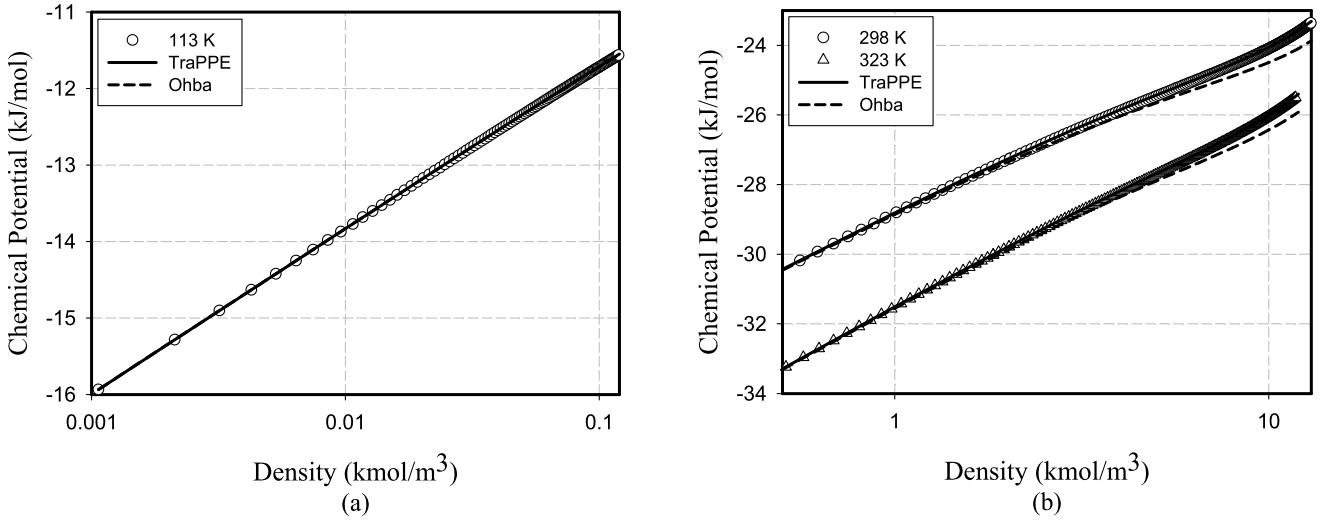

Fig. 3 The bulk behavior of methane at (**a**) 113 (subcritical conditions), (**b**) 298 and 323 K (supercritical conditions)

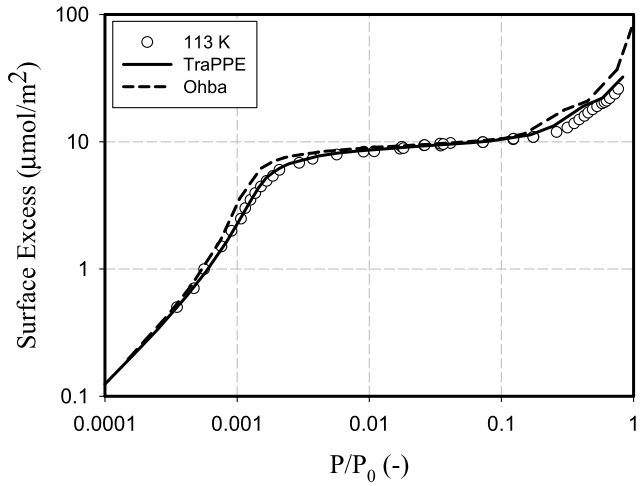

Fig. 4 Adsorption isotherm of methane on graphitized thermal carbon black at 113 K (Avgul and Kiselev 1970)

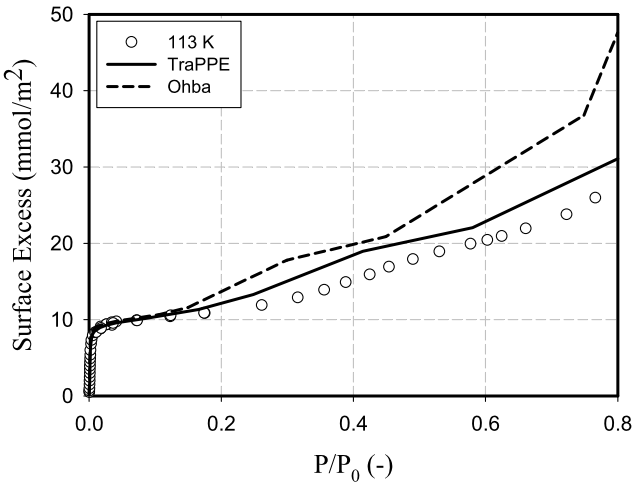

Fig. 5 Adsorption isotherm of methane on graphitized thermal carbon black at 113 K at higher loading (Avgul and Kiselev 1970)

ethylene in the description of VLE and bulk phase behavior and then in the description of adsorption on graphite under sub- and super-critical conditions.

3.1 Methane

3.1.1 Vapor-liquid equilibria and bulk phase behavior

Results of VLE from the Gibbs Ensemble Monte Carlo simulations are shown in Fig. 2 for different potential models. Among these models tested, the TraPPE model is the most satisfactory.

This might be expected since the parameters of TraPPE model were optimized against the VLE data. Other models fail in some descriptions of the experimental data, for example the potential model suggested by Ohba et al. (hereafter called the O-model) fails to describe the co-existence of two phases, due to its relatively large well depth ($\varepsilon/k_B = 161.3$ K). Surprisingly, the atomically detailed model proposed by Sun et al. (5 LJ sites and 5 partial charges) cannot describe the VLE data correctly. This failure to describe the VLE data is also transferred to a poor description of the adsorption data. For clarity we shall take the TraPPE model and the O-model as representative of those describing the VLE data most faithfully and least faithfully respectively.

For the description of the bulk gas behavior, we conducted isobaric-isothermal ensemble Monte Carlo (NPT) simulations to obtain the chemical potential versus density. The simulation results were then compared with the accurate Wagner equation of states (EOS) (Setzmann and Wagner 1991; Smukala et al. 2000). Figure 3 shows the simulation results for 113, 298, and 323 K (the first temperature is below the critical point). These temperatures were selected

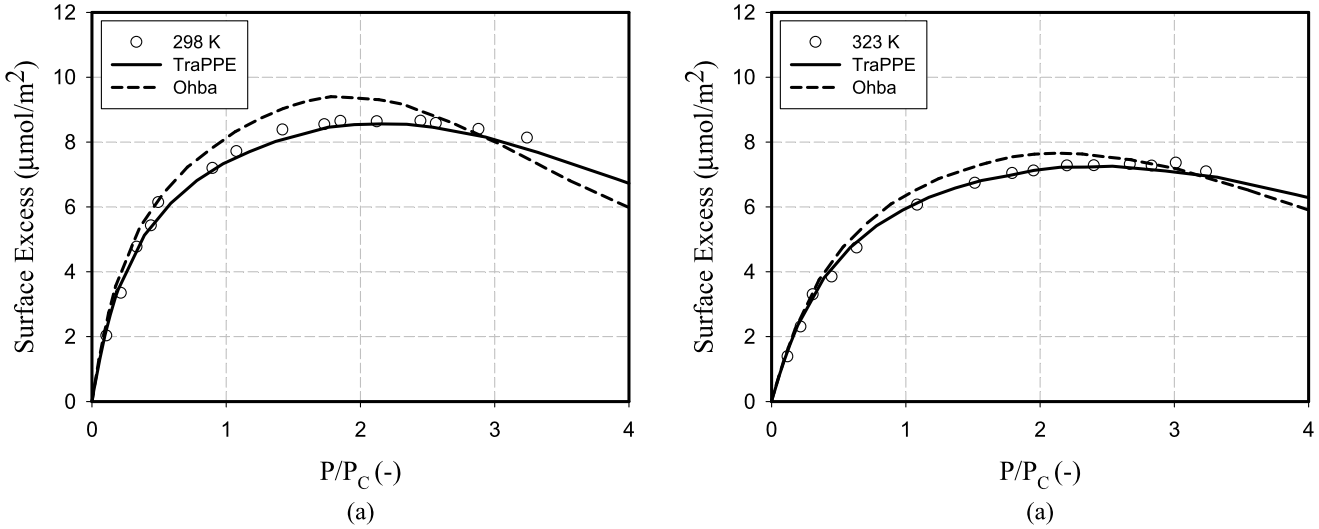

Fig. 6 Adsorption isotherm of methane on graphitized thermal carbon black at 298 and 323 K, plotted against Specovius and Findenegg data (Specovius and Findenegg 1978)

Table 2 The binary interaction parameters at various temperatures for the TraPPE and O-models

	Specovius Data		Our Data	
T (K)	298 K	323 K	288 K	298 K
TraPPE	−0.1	−0.08	0.05	0.05
Ohba	−0.05	−0.01	0.07	0.07

because the adsorption data are available. Like the description of VLE earlier, the TraPPE model description of the bulk phase is very good and is rather poor for the O-model. This has a significant ramification in the calculation of surface excess, and incorrect results for supercritical conditions are expected with the O-model.

3.1.2 Adsorption on graphitized thermal carbon black under subcritical conditions

We compare our model predictions with the experimental data of methane adsorption on graphitized thermal carbon black, Sterling FT(2800) (Avgul and Kiselev 1970). This carbon black has a N_2-BET surface area of 12.2 m^2/g. Because of the difference between the saturation pressures from simulation and experimental data, we plot the adsorption isotherm as the surface excess versus the relative rather than absolute pressure. The results for methane adsorption at 113 K are shown in Fig. 4 on a log-log scale in order to highlight the sub-monolayer region. The O-model fails to describe the experimental data, whereas the agreement between the TraPPE model and the data is better, for reasons that we have mentioned earlier. It is noted that the binary interaction parameters, k_{SF}, are different for different potential models. The k_{SF} applied for the TraPPE and O-model are −0.02 and −0.03, respectively.

To test the suitability of the potential models in the description of the multilayer region, we show in Fig. 5 the simulation results and the data in the linear scale. It is once again found that the TraPPE model describes the multilayer region better than the O-model.

3.1.3 Adsorption on graphitized thermal carbon black under supercritical conditions

Supercritical adsorption isotherms unlike sub-critical isotherms exhibit a maximum. Adsorption data for methane and argon on Graphon under supercritical conditions have been measured by Specovius and Findenegg (1978), and were used to test the simulation results. Here we present only the simulation results of methane; the results for argon are given in the Supplementary Material for reference. To compare the simulation results against the experimental data, we scale the pressure by its respective critical pressure because the critical properties differ between the simulation and the experimental data. The experimental critical properties are taken from NIST (Linstrom and Mallard 2001), and for the simulation are estimated as suggested by Johnson et al. (1993); the LJ-critical pressure being 0.13 (in reduced units). The critical pressures used in this work were 4.61, 5.12, 5.62 MPa for experimental data, TraPPE and O-models, respectively. Figure 6 shows the simulation results

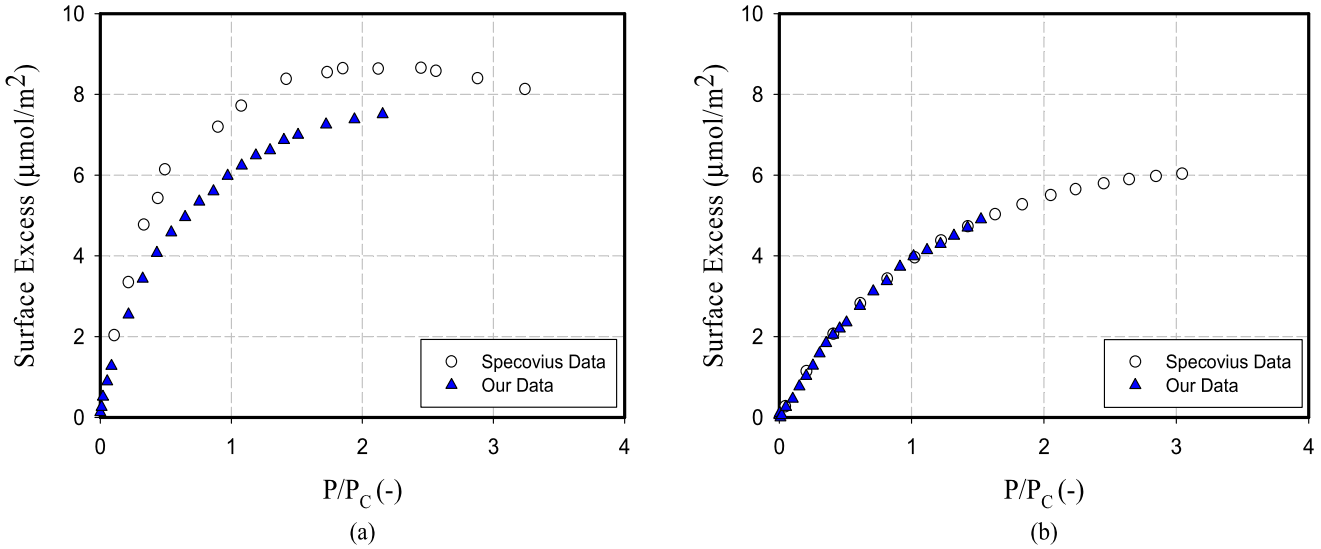

Fig. 7 The comparison between our data with Specovius and Findenegg data for the adsorption isotherm of (**a**) methane and (**b**) argon on graphitized thermal carbon black at 298 K

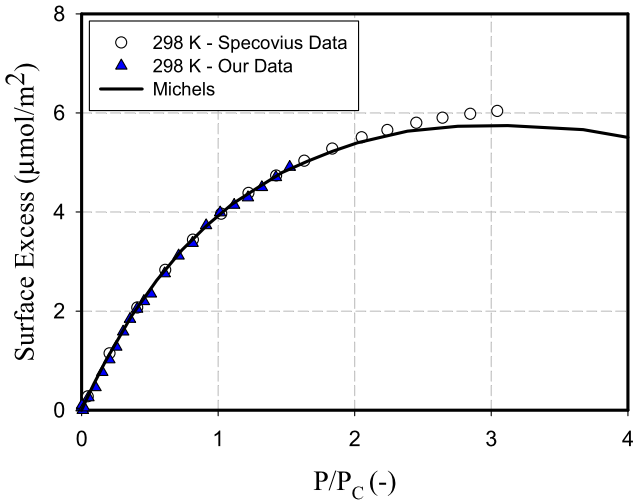

Fig. 8 Adsorption isotherm of argon on graphitized thermal carbon black at 298 K for Michels model. The binary interaction parameter for both temperatures is 0.07

of TraPPE and O-models for methane adsorption at 298 and 323 K and the corresponding experimental data (Specovius and Findenegg 1978). The binary interaction parameter used to match the simulation results and the data in the low pressure region (Henry law region) are listed in Table 2. There is slight disagreement between the simulation results for both models; the data especially at 298 K, from the TraPPE model being the better.

In view of the fact that the simulation results describe the experimental data well under sub-critical conditions, the failure to describe the data under supercritical conditions raises a serious question of why the molecular models fail to describe such a very simple adsorption system since the failure to do so for a simple system can lead to serious doubt about its ability to describe more complex systems. This slight disagreement could either be due to a deficiency in the potential model or that the experimental data are not sufficiently accurate since a small error in the void volume can lead to the wrong surface excess density (Do et al. 2010; Fan et al. 2010). To confirm the accuracy of the experimental data (Specovius and Findenegg 1978), we carried out measurements of methane and argon adsorption on the highly graphitized thermal carbon black (Carbopack F from Supelco) at 288 and 298 K with a high pressure microbalance (BELSORP-BG). The comparison between our experimental isotherm at 298 K and the earlier results is shown in Fig. 7 for methane and for argon. The excellent agreement between our argon results and the earlier experimental data (Fig. 7b) confirms that the discrepancy between experiment and simulation results for argon (Fig. 8) would rest with either the potential model or the deficiency of the simulation method for the description of supercritical adsorption. On the other hand, the disagreement between the two sets of experimental data for methane shown in Fig. 7 suggests that there may be an error in the determination of the void volume in the earlier results. Several points could be made to support this argument: (i) the smoother curve obtained in our data, (ii) the better equipment used in our work, enabled us to control the pressure and temperature more accurately and (iii) the high negative value of k_{SF} necessary to fit the literature data (because of the possible over-determination of the experimental adsorption excess). Normally this parameter is very small when determined for sub-critical adsorption.

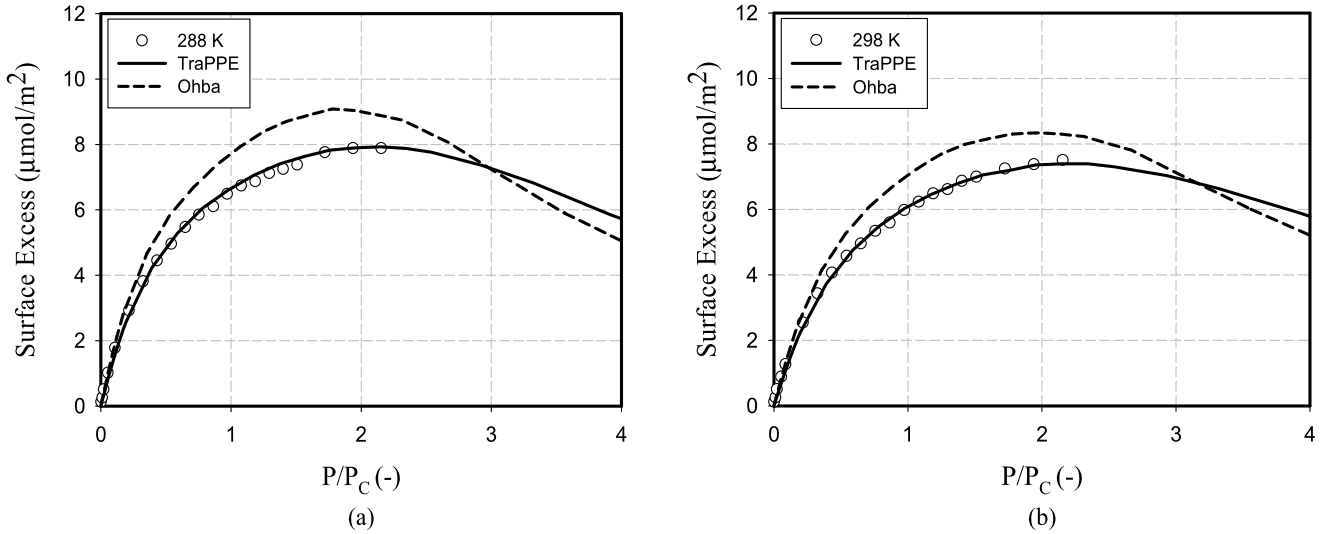

Fig. 9 Adsorption isotherm of methane on graphitized thermal carbon black at 288 and 298 K, plotted against our experimental data

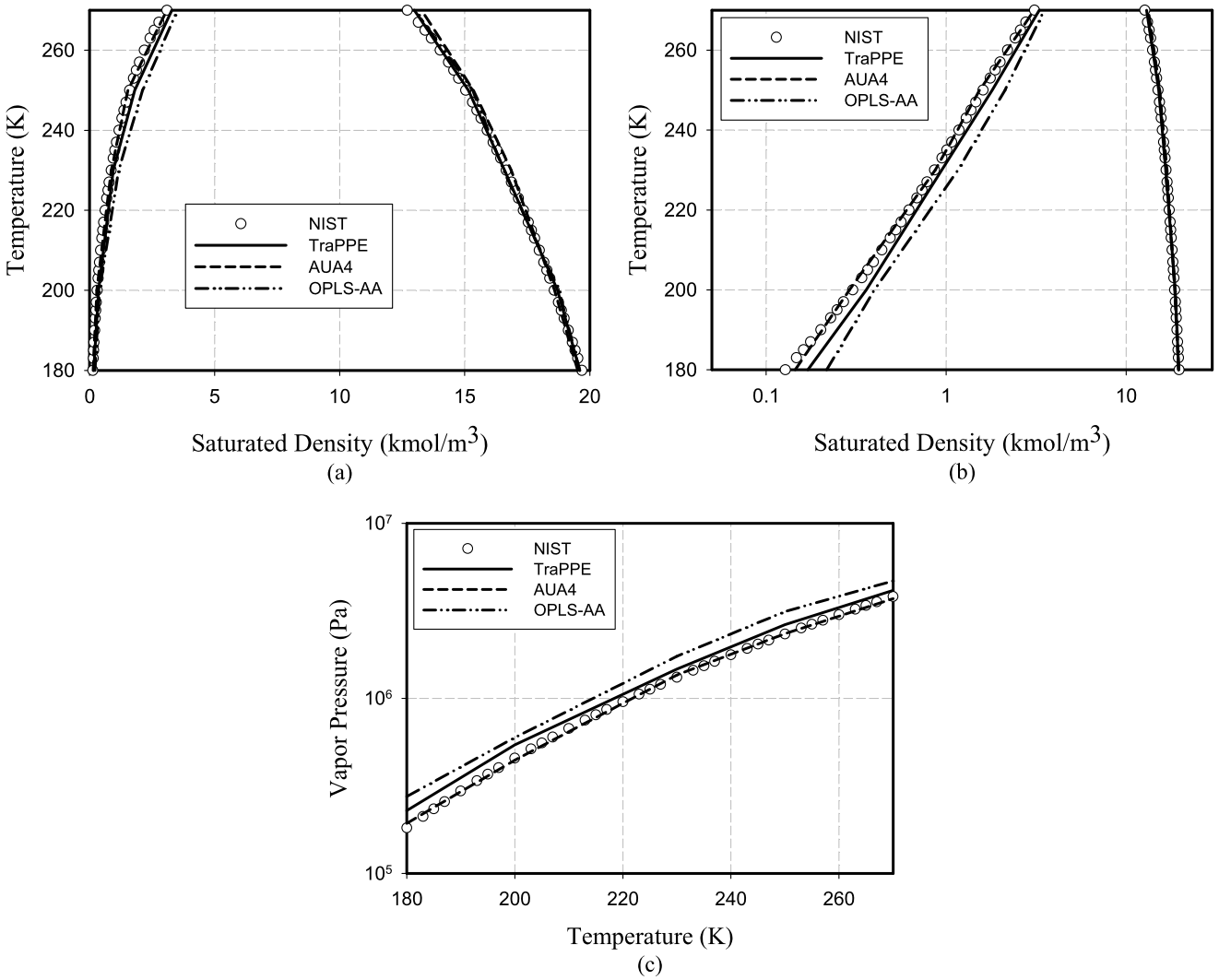

Fig. 10 VLE phase diagrams for ethylene: (**a**) linear scale of density (*top LHS*) and (**b**) log scale of density (*top RHS*), (**c**) vapor pressures versus temperatures (*bottom*)

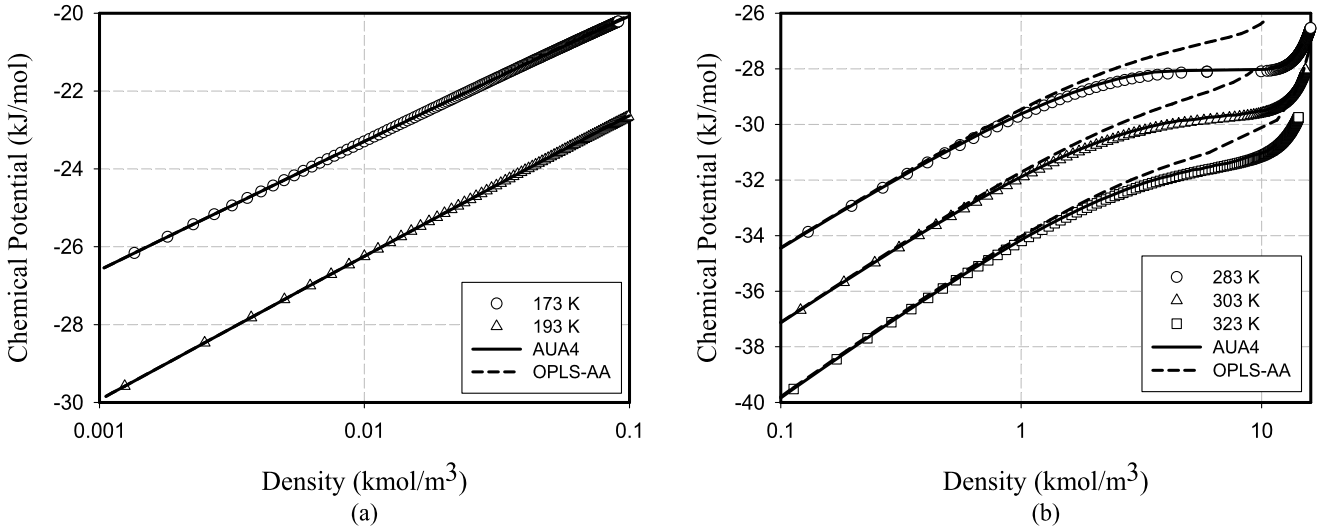

Fig. 11 The bulk behavior of ethylene at (**a**) 173 and 193 K (subcritical conditions), (**b**) 283 (near-critical conditions), 303, and 323 K (supercritical conditions)

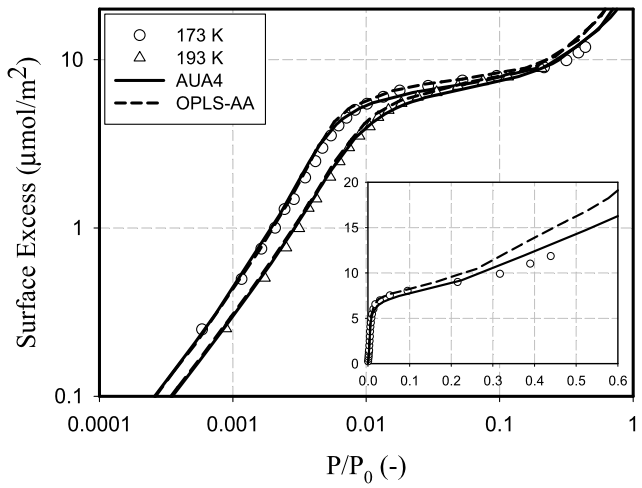

Fig. 12 Adsorption isotherm of ethylene on graphitized thermal carbon black at 173, and 193 K (Avgul and Kiselev 1970). The *inset* shows the linear scale plot at 173 K to illustrate the description of the higher loading

Figure 9 shows the simulation results for TraPPE and O-models for methane adsorption at 288 and 298 K and our experimental data. Interestingly, the TraPPE model describes the data very well using smaller k_{SF} given in Table 2, which further supports the argument that the void volume in the literature data might be incorrectly determined. However, due to the limitation in the available pressure range of our equipment, we could not obtain a clear maximum excess. To investigate further, we consider ethylene next as its experimental data show a clear and sharp maximum in the plot of the excess density versus pressure when temperatures are close to the critical point.

3.2 Ethylene

3.2.1 Vapor-liquid equilibria and bulk phase behavior

For ethylene, we considered six sets of molecular parameters which have been proposed in the literature (Table 1). With the exception of the OPLS-AA model (which explicitly accounts for all atoms and partial charges), all the models treat ethylene as a collection of two united atoms (CH_2) (Ryckaert and Bellemans 1978). The Vrabec model has an additional point quadrupole located between the two united atoms.

Figure 10 shows the of vapor-liquid equilibrium (VLE) curves from the TraPPE, AUA-4 and OPLS-AA models (VLE results for other models are available in the Supplementary Material). The OPLS-AA, where the molecular parameters are not optimized against the VLE data, give the worst agreement, and AUA-4 the best.

The bulk fluid results obtained from the isobaric-isothermal ensemble Monte Carlo (NPT) simulations are compared with the accurate Wagner equation of states (EOS) (Setzmann and Wagner 1991; Smukala et al. 2000) in Fig. 11. The figure shows results for chemical potential versus density at 173, 193, 283, 303 and 323 K obtained with the OPLS-AA and AUA-4 models. Both models describe the bulk fluid under sub-critical conditions well, but only the AUA-4 is satisfactory under supercritical conditions. The failure of the OPLS-AA model in its description of VLE and the bulk fluid is translated to the poor description of adsorption data as we shall show next.

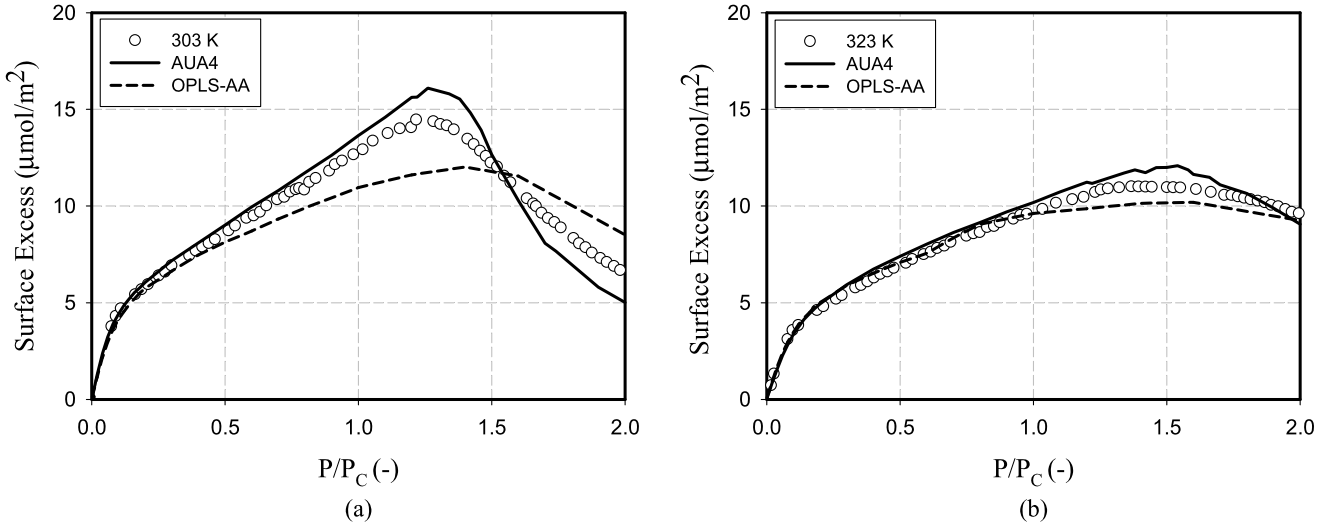

Fig. 13 Adsorption isotherm of ethylene on graphitized thermal carbon black at 303 and 323 K, plotted against Specovius and Findenegg data (Specovius and Findenegg 1980)

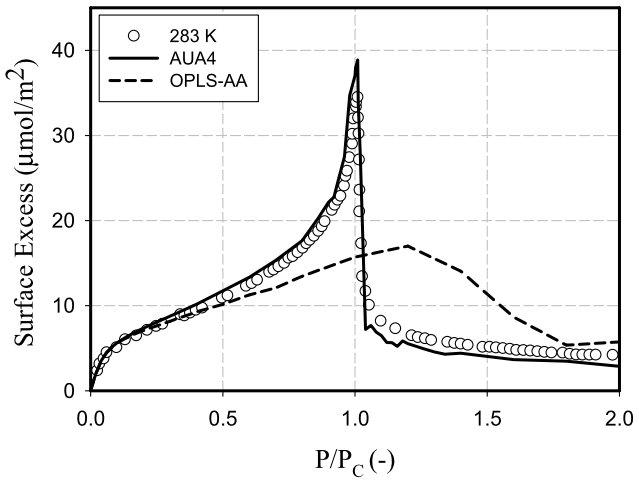

Fig. 14 Adsorption isotherm of ethylene on graphitized thermal carbon black at 283 K, plotted against Specovius and Findenegg data (Specovius and Findenegg 1980)

3.2.2 Adsorption on graphitized thermal carbon black under subcritical conditions

The comparison between the simulation results obtained from the AUA-4 and OPLS-AA models and the experimental data of Avgul and Kiselev at 173 and 193 K is shown in Fig. 12 on a log-log scale. The two models describe the data reasonably well over the sub-monolayer region, but the description of the second layer is better with the AUA-4 model. This reinforces our earlier argument that good description of VLE of a potential model leads to a good description of adsorption on a surface.

3.2.3 Adsorption on graphitized thermal carbon black under supercritical conditions

Experimental data under supercritical and near-critical conditions available in the literature (Specovius and Findenegg 1980), were used to test the molecular models. The simulation results, from the AUA-4 and OPLS-AA models are presented in Fig. 13 together with the experimental data at 303 and 323 K. The results show that the AUA-4 model could describe the experimental data reasonably well especially the position of the maximum in the adsorption excess. However the OPLS-AA gives rather poor agreement with experiment which can be attributed to the failure of this model to describe the VLE and the bulk phase data.

3.2.4 Adsorption on graphitized thermal carbon black near critical points

The experimental data for ethylene adsorption on Graphon from Specovius and Findenegg (1980) provide a critical test for potential models because they exhibit a very sharp maximum at 283 K, which is just above the critical temperature (282.35 K). Figure 14 shows the simulation results using AUA-4 and OPLS-AA models and the experimental data. The AUA-4 model is in remarkably good agreement with experiment matching both the position and magnitude of this spike. The maximum from the OPLS-AA model is lower and displaced to higher pressure even though it accounts explicitly for all atoms in the molecule since the parameters are not optimized as remarked earlier.

4 Conclusions

In this paper we have presented a simulation study of methane and ethylene adsorption on a graphite surface under sub-critical and supercritical conditions with various potential models. Under supercritical conditions, the simulation results for potential models that describe the VLE and bulk phase well were also found to give a good description of the experimental adsorption isotherms, provided that the adsorption data and the void volume are accurately determined. These requirements are not so stringent at subcritical temperatures because of the very low bulk density compared to the density of the adsorbed phase.

We conclude that in order to achieve an accurate description of adsorption, a potential model needs to be optimized against the bulk fluid behavior and the VLE, and that the experimental data must be obtained correctly and accurately.

Acknowledgements This project is supported by the Australian Research Council.

References

Abdul Razak, M.a., Do, D., Birkett, G.: Evaluation of the interaction potentials for methane adsorption on graphite and in graphitic slit pores. Adsorption **17**(2), 385–394 (2011)

Agarwal, R.K., Schwarz, J.A.: Analysis of high-pressure adsorption of gases on activated carbon by potential-theory. Carbon **26**(6), 873–887 (1988)

Allen, M.P., Tildesley, D.J.: Computer Simulation of Liquids, p. 385. Oxford University Press, Oxford (1989)

Aranovich, G.L., Donohue, M.D.: Adsorption of supercritical fluids. J. Colloid Interface Sci. **180**(2), 537–541 (1996)

Avgul, N.N., Kiselev, A.V.: Physical adsorption of gases and vapous on graphitized carbon blacks. Chem. Phys. Carbon **6**, 1–124 (1970)

Bourasseau, E., Haboudou, M., Boutin, A., Fuchs, A.H., Ungerer, P.: New optimization method for intermolecular potentials: optimization of a new anisotropic united atoms potential for olefins: prediction of equilibrium properties. J. Chem. Phys. **118**(7), 3020–3034 (2003)

Darkrim, F., Vermesse, J., Malbrunot, P., Levesque, D.: Monte Carlo simulations of nitrogen and hydrogen physisorption at high pressures and room temperature. Comparison with experiments. J. Chem. Phys. **110**(8), 4020–4027 (1999)

Darkrim, F.L., Malbrunot, P., Tartaglia, G.P.: Review of hydrogen storage by adsorption in carbon nanotubes. Int. J. Hydrog. Energy **27**(2), 193–202 (2002)

Do, D.D., Do, H.D.: Adsorption of argon from sub- to supercritical conditions on graphitized thermal carbon black and in graphitic slit pores: a grand canonical Monte Carlo simulation study. J. Chem. Phys. **123**(8) (2005a)

Do, D.D., Do, H.D.: Effects of potential models in the vapor–liquid equilibria and adsorption of simple gases on graphitized thermal carbon black. Fluid Phase Equilib. **236**(1,2), 169–177 (2005b)

Do, D.D., Do, H.D.: Adsorption of argon on homogeneous graphitized thermal carbon black and heterogeneous carbon surface. J. Colloid Interface Sci. **287**(2), 452–460 (2005c)

Do, D.D., Do, H.D., Nicholson, D.: A computer appraisal of BET theory, BET surface area and the calculation of surface excess for gas adsorption on a graphite surface. Chem. Eng. Sci. **65**(10), 3331–3340 (2010)

El-Merraoui, M., Aoshima, M., Kaneko, K.: Micropore size distribution of activated carbon fiber using the density functional theory and other methods. Langmuir **16**(9), 4300–4304 (2000)

Fan, C.Y., Herrera, L.F., Do, D.D., Nicholson, D.: New method to determine surface area and its energy distribution for nonporous solids: a computer simulation and experimental study. Langmuir **26**(8), 5610–5623 (2010)

Frenkel, D., Smit, B.: Understanding Molecular Simulation: From Algorithms to Applications, p. 443. Academic Press, San Diego (1996)

Gao, W.H., Butler, D., Tomasko, D.L.: High-pressure adsorption of CO_2 on NaY zeolite and model prediction of adsorption isotherms. Langmuir **20**(19), 8083–8089 (2004)

Hocker, T., Rajendran, A., Mazzotti, M.: Measuring and modeling supercritical adsorption in porous solids. Carbon dioxide on 13X zeolite and on silica gel. Langmuir **19**(4), 1254–1267 (2003)

Jiang, S.Y., Zollweg, J.A., Gubbins, K.E.: High-pressure adsorption of methane and ethane in activated carbon and carbon-fibers. J. Phys. Chem. **98**(22), 5709–5713 (1994)

Johnson, J.K., Zollweg, J.A., Gubbins, K.E.: The Lennard-Jones equation of state revisited. Mol. Phys. **78**(3), 591–618 (1993)

Jorgensen, W.L., Maxwell, D.S., TiradoRives, J.: Development and testing of the OPLS all-atom force field on conformational energetics and properties of organic liquids. J. Am. Chem. Soc. **118**(45), 11225–11236 (1996)

Kaneko, K., Murata, K.: An analytical method of micropore filling of a supercritical gas. Adsorption **3**(3), 197–208 (1997)

Kowalczyk, P., Tanaka, H., Kaneko, K., Terzyk, A.P., Do, D.D.: Grand canonical Monte Carlo simulation study of methane adsorption at an open graphite surface and in slitlike carbon pores at 273 K. Langmuir **21**(12), 5639–5646 (2005)

Linstrom, P.J., Mallard, W.G.: NIST Chemistry WebBook (2001). Available from: http://webbook.nist.gov

Liu, Z.J., Do, D.D., Nicholson, D.: Effects of confinement on the molar enthalpy of argon adsorption in graphitic cylindrical pores: a grand canonical Monte Carlo (GCMC) simulation study. J. Colloid Interface Sci. **361**(1), 278–287 (2011)

Malbrunot, P., Vidal, D., Vermesse, J., Chahine, R., Bose, T.K.: Adsorption measurements of argon, neon, krypton, nitrogen, and methane on activated carbon up to 650 MPa. Langmuir **8**(2), 577–580 (1992)

Malbrunot, P., Vidal, D., Vermesse, J.: Storage of gases at room temperature by adsorption at high pressure. Appl. Therm. Eng. **16**(5), 375–382 (1996)

Martin, M.G., Siepmann, J.I.: Transferable potentials for phase equilibria. I. United-atom description of *n*-alkanes. J. Phys. Chem. B **102**(14), 2569–2577 (1998)

Matranga, K.R., Myers, A.L., Glandt, E.D.: Storage of natural gas by adsorption on activated carbon. Chem. Eng. Sci. **47**(7), 1569–1579 (1992)

Menon, P.G.: Adsorption at high pressures. Chem. Rev. **68**, 277–294 (1968)

Michels, A., Wijker, H., Wijker, H.: Isotherms of argon between 0 °C and 150 °C and pressures up to 2900 atmospheres. Physica **15**(7), 627–633 (1949)

Murata, K., El-Merraoui, M., Kaneko, K.: A new determination method of absolute adsorption isotherm of supercritical gases under high pressure with a special relevance to density-functional theory study. J. Chem. Phys. **114**(9), 4196–4205 (2001)

Nath, S.K., Banaszak, B.J., de Pablo, J.J.: A new united atom force field for alpha-olefins. J. Chem. Phys. **114**(8), 3612–3616 (2001)

Nguyen, V.T., Do, D.D., Nicholson, D.: On the heat of adsorption at layering transitions in adsorption of noble gases and nitrogen on graphite. J. Phys. Chem. C **114**(50), 22171–22180 (2010)

Nicholson, D., Parsonage, G.: Computer Simulation and the Statistical Mechanics of Adsorption, p. 398. Academic Press, London (1982)

Ohba, T., Omori, T., Kanoh, H., Kaneko, K.: Cluster structures of supercritical CH_4 confined in carbon nanospaces with in situ high-pressure small-angle X-ray scattering and grand canonical Monte Carlo simulation. J. Phys. Chem. B **108**(1), 27–30 (2004)

Ozawa, S., Kusumi, S., Ogino, Y.: Physical adsorption of gases at high-pressure. IV. Improvement of Dubinin-Astakhov adsorption equation. J. Colloid Interface Sci. **56**(1), 83–91 (1976)

Panagiotopoulos, A., Quirke, N., Stapleton, M., Tildesley, D.J.: Phase equilibria by simulation in the Gibbs ensemble: alternative derivation, generalization and application to mixtures and membrane equilibria. Mol. Phys. **63**, 527–545 (1988)

Poirier, E., Chahine, R., Bose, T.K.: Hydrogen adsorption in carbon nanostructures. Int. J. Hydrog. Energy **26**(8), 831–835 (2001)

Ryckaert, J., Bellemans, A.: Molecular dynamics of liquid alkanes. Faraday Discuss. Chem. Soc. **66**, 95–106 (1978)

Salem, M.M.K., Braeuer, P., von Szombathely, M., Heuchel, M., Harting, P., Quitzsch, K., Jaroniec, M.: Thermodynamics of high-pressure adsorption of argon, nitrogen, and methane on microporous adsorbents. Langmuir **14**(12), 3376–3389 (1998)

Setzmann, U., Wagner, W.: A new equation of state and tables of thermodynamic properties for methane covering the range from the melting line to 625 K at pressure up to 1000 MPa. J. Phys. Chem. **20**(6), 1061–1155 (1991)

Smukala, J., Span, R., Wagner, W.: New equation of state for ethylene covering the fluid region for temperatures from the melting line to 450 K at pressures up to 300 MPa. J. Phys. Chem. Ref. Data **29**(5), 1053–1121 (2000)

Specovius, J., Findenegg, G.H.: Physical adsorption of gases at high-pressure: argon and methane onto graphitized carbon black. Ber. Bunsenges. Phys. Chem. **82**(2), 174–180 (1978)

Specovius, J., Findenegg, G.H.: Study of a fluid-solid interface over a wide density range including the critical region. I. Surface excess of ethylene-graphite. Ber. Bunsenges. Phys. Chem. **84**(7), 690–696 (1980)

Spyriouni, T., Economou, I.G., Theodorou, D.N.: Phase equilibria of mixtures containing chain molecules predicted through a novel simulation scheme. Phys. Rev. Lett. **80**(20), 4466–4469 (1998)

Steele, W.A.: The physical interaction of gases with crystalline solids: I. Gas-solid energies and properties of isolated adsorbed atoms. Surf. Sci. **36**(1), 317–352 (1973)

Sun, Y.X., Spellmeyer, D., Pearlman, D.A., Kollman, P.: Simulation of the solvation free-energies for methane, ethane, and propane and corresponding amino-acid dipertides—a critical test of the bond-PMF correction, a new set of hydrocarbon parameters, and the gas-phase water hydrophobicity scale. J. Am. Chem. Soc. **114**(17), 6798–6801 (1992)

Tan, Z., Gubbins, K.E.: Adsorption in carbon micropores at supercritical temperatures. J. Phys. Chem. **94**(15), 6061–6069 (1990)

Tanaka, H., El-Merraoui, M., Kodaira, T., Kaneko, K.: Possibility of quantum effect in micropore filling of Ne on AlPO4-5. Chem. Phys. Lett. **351**(5–6), 417–423 (2002)

Ustinov, E.A.: Modeling of N2 adsorption in MCM-41 materials: hexagonal pores versus cylindrical pores. Langmuir **25**(13), 7450–7456 (2009)

Ustinov, E.A., Do, D.D.: High-pressure adsorption of supercritical gases on activated carbons: an improved approach based on the density functional theory and the bender equation of state. Langmuir **19**(20), 8349–8357 (2003)

Vrabec, J., Stoll, J., Hasse, H.: A set of molecular models for symmetric quadrupolar fluids. J. Phys. Chem. B **105**(48), 12126–12133 (2001)

Wick, C.D., Martin, M.G., Siepmann, J.I.: Transferable potentials for phase equilibria. 4. United-atom description of linear and branched alkenes and alkylbenzenes. J. Phys. Chem. B **104**(33), 8008–8016 (2000)

Zhou, L., Zhou, Y., Bai, S., Yang, B.: Studies on the transition behavior of physical adsorption from the sub- to the supercritical region: experiments on silica gel. J. Colloid Interface Sci. **253**(1), 9–15 (2002)